ISSN 1063-7761, Journal of Experimental and Theoretical Physics, 2009, Vol. 108, No. 1, pp. 48–55. © Pleiades Publishing, Inc., 2009.
Original Russian Text © G.A. Ovsyannikov, A.M. Petrzhik, I.V. Borisenko, A.A. Klimov, Yu.A. Ignatov, V.V. Demidov, S.A. Nikitov, 2009, published in Zhurnal Éksperimental'noĭ i Teoreticheskoĭ Fiziki, 2009, Vol. 135, No. 1, pp. 56–64.

ORDER, DISORDER, AND PHASE TRANSITION IN CONDENSED SYSTEMS

Magnetotransport Characteristics of Strained $La_{0.7}Sr_{0.3}MnO_3$ Epitaxial Manganite Films

G. A. Ovsyannikov[a, b, *], A. M. Petrzhik[a], I. V. Borisenko[a], A. A. Klimov[a], Yu. A. Ignatov[a], V. V. Demidov[a], and S. A. Nikitov[a]

[a] *Institute of Radio-Engineering and Electronics, Russian Academy of Sciences, Mokhovaya 11, Moscow, 125009 Russia*
** e-mail: gena@hitech.cplire.ru*
[b] *Chalmers University of Technology, Göteborg, SE-41296 Sweden*

Received April 4, 2008

Abstract—The electrical and magnetic characteristics of $La_{0.7}Sr_{0.3}MnO_3$ (LSMO) epitaxial manganite films are investigated by different methods under conditions when the crystal structure is strongly strained as a result of mismatch between the lattice parameters of the LSMO crystal and the substrate. Substrates with lattice parameters larger and smaller than the nominal lattice parameter of the LSMO crystal are used in experiments. It is shown that the behavior of the temperature dependence of the electrical resistance for the films in the low-temperature range does not depend on the strain of the film and agrees well with the results obtained from the calculations with allowance made for the interaction of electrons with magnetic excitations in the framework of the double-exchange model for systems with strongly correlated electronic states. Investigations of the magneto-optical Kerr effect have revealed that an insignificant (0.3%) orthorhombic distortion of the cubic lattice in the plane of the $NdGaO_3$(110) substrate leads to uniaxial anisotropy of the magnetization of the film, with the easy-magnetization axis lying in the substrate plane. However, LSMO films on substrates (($(LaAlO_3)_{0.3}$ + $(Sr_2AlTaO_6)_{0.7}$)(001)) ensuring minimum strain of the films exhibit a biaxial anisotropy typical of cubic crystals. The study of the ferromagnetic resonance lines at a frequency of 9.76 GHz confirms the results of magneto-optical investigations and indicates that the ferromagnetic phase in the LSMO films is weakly inhomogeneous.

PACS numbers: 74.45.+c, 74.50.+r, 75.70.Cn

DOI: 10.1134/S1063776109010075

1. INTRODUCTION

Rare-earth manganite perovskites $Re_{1-x}A_xMnO_3$ (where *Re* is a rare-earth element of the La or Nd type and *A* is an alkaline-earth metal of the Sr or Ca type) exhibit a wide spectrum of unusual electrical and magnetic properties, including the colossal magnetoresistance effect (see reviews [1–4]). The parameters of epitaxial films of these materials very often differ substantially from the characteristics of single crystals. As was shown in a number of works [2, 3, 5–12], the factor responsible for the change in the electrical and magnetic parameters is a strain arising in the films due to the mismatch with the substrate used for depositing the film. It was demonstrated that the three-dimensional compression of the crystal lattice increases the hopping probability amplitude within the double-exchange model, which results in an increase in the Curie temperature T_C [12], whereas biaxial distortions of the Jahn–Teller type lead to an enhancement of electron localization and decrease the Curie temperature T_C [5, 6, 11]. The magnetic properties of films are substantially affected by the phase separation phenomena and the presence of a nonmagnetic layer at the substrate–film interface [9]. These effects most strongly manifest themselves in very thin films (thinner than 10 nm). However, a number of problems associated with the influence of the strain on the electrical and magnetic properties of LSMO films have remained unclear and call for further investigation. There is no experimentally confirmed model of the temperature dependence of the electrical resistance for films at low temperatures [4], the problems regarding the influence of the film strain on the magnetic anisotropy [3] and the Curie temperature [5, 6] remain unsolved, etc.

In the present paper, we described the results of combined experimental investigation of epitaxial $La_{0.7}Sr_{0.3}MnO_3$ (LSMO) films deposited onto substrates with different crystal lattice parameters. We chose substrates for which the mismatch between the crystal lattice parameters of the substrate and the LSMO film varied from –2.2 to 2.0%. Owing to the use of identical deposition conditions, it was possible to avoid the effect of other factors (except for the film strain) on the magnetotransport characteristics of films. The film thickness exceeded the thickness (3–5 nm) of the "dead" (nonmagnetic) layer at the film–substrate interface [3, 9] but was smaller than the critical thickness (on the order of 100 nm) at which the strain relaxation is observed in the film. The electrical conductivity, the ferromagnetic transition temperature, and the

magnetization anisotropy of the films were studied as a function of the strain induced in the manganite films by interaction with the substrate.

2. SAMPLE PREPARATION AND EXPERIMENTAL TECHNIQUE

Epitaxial LSMO films 40–100 nm thick were deposited onto $LaAlO_3(001)$ (LAO), $SrTiO_3(001)$ (STO), $NdGaO_3(110)$ (NGO), $((LaAlO_3)_{0.3} + (Sr_2AlTaO_6)_{0.7})(001)$ (LSAT), $GdSrO_3(110)$ (GSO), and $DyScO_3(110)$ (DSO) substrates by laser ablation (KrF laser, $\lambda = 248$ nm) at a temperature of 600–800°C and an oxygen pressure of 0.2 mbar.[1] All films were cooled under identical conditions (10°C/min, atmospheric pressure) in order to avoid a variation in the oxygen content in the films.[2]

The crystallographic parameters of the films and substrates were determined by measuring the X-ray diffraction patterns ($2\theta/\omega$ and φ scan mode) and the rocking curves on a four-circle X-ray diffractometer.

The resistance of the films was measured by the four-point probe method, which excluded the influence of the contact resistance. Contact electrodes were applied by sputtering of platinum through a metal mask.

The presence of the ferromagnetic phase in the LSMO films at room temperature makes it possible to investigate the magnetic parameters with the use of the meridional Kerr effect without additional cooling, which simplifies the measurements of the spatial anisotropy of magnetic parameters. The magneto-optical setup for measuring the characteristics of the samples consists of a semiconductor laser ($\lambda = 0.63$ μm, $P = 5$ mW), a beam-splitting glass plate for the formation of the reference and signal beams, a phase half-wave plate for the selection of the *s* or *p* polarization of light incident on the sample, a polarizer–analyzer for the separation of the signal associated with the meridional Kerr effect, and two photodiodes, one of which is located in the reference channel and the other diode is positioned in the signal channel. The photodiodes operating in the bias mode are connected to a differential resonance amplifier tuned to the frequency of modulation of the laser radiation intensity. The signal (proportional to the change in the angle of rotation of the plane of polarization of reflected light) is fed from the differential amplifier to an analog-to-digital converter (NI6221) and then is processed with the LabView software package. The sample to be studied is located on a rotary table in the gap of an electromagnet. In the setup, the sample can be rotated around the normal to the substrate plane by an angle in the range 0°–360°.

The magnetic characteristics were also measured using the magnetic resonance method. The magnetic resonance spectra were recorded on a Bruker ER-200 EPR spectrometer operating in the 3-cm range of electromagnetic waves (frequency, 9.76 GHz). The signal recording was performed by synchronous detection at the frequency of modulation of the external magnetic field (100 kHz). The samples under investigation were located in a microwave cavity of the spectrometer so that the plane of the sample was always parallel to the direction of the constant external magnetic field and the magnetic component of the microwave field. The parallelism of the plane of the samples to the constant magnetic field was controlled from the minimum of the resonance field of the ferromagnetic resonance lines. This location of the samples excludes the change in the magnetic resonance spectra due to the anisotropy of the shape. The samples were rotated around the axis perpendicular to the plane of the samples.

3. CRYSTALLOGRAPHIC INVESTIGATIONS

The grown LSMO films were precisely oriented with respect to both the normal to the plane of the substrate and the preferred direction in the plane of the substrate. The interplanar distance $a_\perp$ in the LSMO films along the normal to the plane of the substrate and the lattice constant a_s of the substrate were determined from the X-ray diffraction patterns (measured in the $2\theta/\omega$ scan mode). Figure 1 shows the X-ray diffraction patterns (measured in the $2\theta/\omega$ scan mode) of the LSMO/NGO and LSMO/STO films. It can be seen from Fig. 1 that the parameter $a_\perp$ of the LSMO film depends strongly on the parameter a_s of the substrate (see also the inset to Fig. 1). The dashed line indicates the position of the hypothetical reflection (002) LSMO for the bulk material (without regard for strains) with the unit cell parameter (in the pseudocubic representation) $a_{LSMO} = 0.3876$ nm obtained from the measurements of LSMO polycrystals [12]. The lattice constant (coinciding within the limits of experimental error) of individual LSMO film was determined from the experimental data presented in the inset to Fig. 1, which depicts the dependence of the measured interplanar distance $a_\perp$ of the LSMO films on the lattice parameter a_s of the substrates. These parameters were determined from the (002), (003), and (004) peaks of the LSMO films and substrates. The intersection of the dependence $a_\perp(a_s)$ with the straight line $a_\perp = a_s$ leads to the lattice constant of the LSMO film $a_{LSMO} = 0.387 \pm 0.014$ nm, which, within the limits of experimental error, coincides with the results obtained in [12]. It is assumed that the lattice constant $a_\parallel$ of the LSMO film in the plane of the substrate coincides with the lattice constant a_s to within the experimental error. This is confirmed by the results of investigations of oblique cross

[1] For the most part, the substrates were manufactured by CrysTec GmbH (Germany).

[2] The results of low-temperature measurements of the resistance of the LSMO films deposited onto the DSO substrates were irreproducible, probably due to cracking of the films upon cooling. In this paper, we do not discuss the results of the measurements performed for these films.

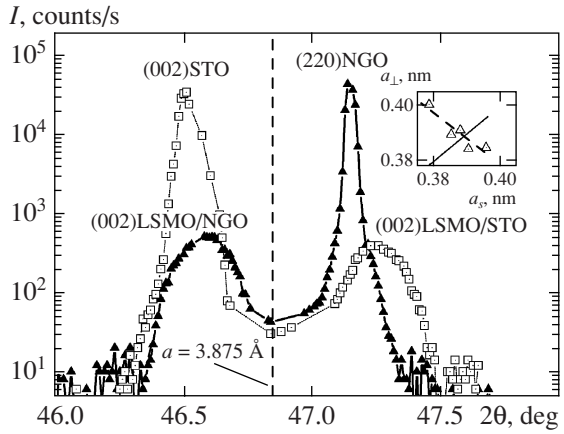

Fig. 1. X-ray diffraction patterns (measured in the 2θ/ω scan mode) of the LSMO films deposited onto the NGO and STO substrates. The dashed line indicates the position of the hypothetical reflection (002)LSMO for the bulk material (without regard for strains) [12]. The corresponding lattice parameter a_{LSMO} within the experimental error coincides with the lattice parameter obtained from the intersection of two lines (solid and dashed) in the inset to the figure, which depicts the dependence of the interplanar distance $a_\perp$ of the LSMO films on the lattice parameter a_s of the substrates.

sections for thin (less than 100 nm) films and the data obtained in [5]. Consequently, the grown manganite films are under the action of the mechanical strains induced by interaction with the substrate: the compressive strains for the NGO and LAO substrates and the tensile strains for the STO, LSAT, and GSO substrates. The biaxial strains in the plane of the substrate lead to a distortion in the crystal lattice of the film in the perpendicular direction.

The strains arising in the film in the plane of the substrate $\varepsilon_\parallel = (a_\parallel - a_{LSMO})/a_{LSMO}$ and in the perpendicular direction $\varepsilon_\perp = (a_\perp - a_{LSMO})/a_{LSMO}$ are listed in the Table 1. The values of the effective volume $V_{eff} = a_\parallel^2 a_\perp$ are also presented in this table. It can be seen from Table 1 that the compressive strains in the plane of the substrate for the LSMO films deposited onto the NGO and LAO substrates increase the interplanar distance $a_\perp$, whereas the tensile strains (for the STO substrates) decrease this interplanar distance. The accuracy in determining the lattice parameters with allowance made for possible tetragonal distortions is equal to 10^{-3} nm in the plane of the substrate and 10^{-4} nm in the perpendicular direction. Therefore, the corresponding errors in the calculations of the strains in the plane of the substrate and in the perpendicular direction are equal to 0.20 and 0.02%, respectively.

It should be noted that the volume V_{eff} of the crystal lattice V_{eff} of the LSMO film is not retained with a change in the substrate. At small lattice distortions, the Curie temperature T_C and other magnetotransport parameters of manganites depend on two parameters: the relative change in the unit cell volume $\varepsilon_b = 2\varepsilon_\parallel + \varepsilon_\perp$ and the biaxial distortion $\varepsilon^* = (\varepsilon_\perp - \varepsilon_\parallel)\sqrt{2/3}$ [6, 11]. The volume distortions of the lattice lead to a decrease or an increase in the Curie temperature T_C depending on the distortion sign, whereas the biaxial distortions always result in a decrease in the Curie temperature T_C. Below, experimental changes in the Curie temperature T_C will be more thoroughly compared with the model [11] which is applicable to small distortions of the cubic lattice.

4. ELECTRICAL PARAMETERS

The resistance of all the films under investigation decreases drastically with a decrease in the temperature $T < T_C$. At low temperatures ($T < 10$ K), the resistivity of all samples approaches the asymptotic value $\rho = \rho_0$. The term ρ_0 independent of the temperature is determined by the processes of scattering from impurities, defects, grain boundaries, and domain walls [13–16]. The minimum resistivity $\rho_0 \approx 8 \times 10^{-5}\ \Omega$ cm is observed for the LSMO/NGO and LSMO/LSAT films, which have the most perfect crystal structure (minimum $\Delta\omega$). The values obtained do not exceed $\rho_0 = 1.1 \times 10^{-4}\ \Omega$ cm for high-quality LSMO/LSAT films [13] but are somewhat larger than those for single crystals [4]. An increase in the quantity ρ_0 for the LSMO/LAO films can be associated with the twinning of the substrate, which results in a broadening of the rocking curve (see Table 1); however, the factors responsible for the increase in the quantity ρ_0 for the LSMO/STO films were not revealed. It should be noted that the rocking curves for the LSMO/STO and LSMO/NGO films coincide with each other, which suggests a high crystallographic quality of the LSMO/STO structures (see

Table 1. Crystallographic parameters of films

Substrate	a_s, nm	$a_\perp$, nm	Δω, deg	V_{eff}, nm^3	$\varepsilon_\perp$, %	$\varepsilon_\parallel$, %	ε_b, %	ε*, %
NGO	0.3862	0.3906	0.06	0.058	0.78	–0.34	–0.10	0.53
LAO	0.3787	0.4003	0.15	0.057	3.28	–2.30	–1.32	2.63
STO	0.3903	0.3845	0.05	0.059	–0.80	0.70	0.59	–0.71
LSAT	0.38748	0.38753	0.06	0.058	–0.02	–0.03	–0.08	0.01
GSO	0.3958	0.3836	0.36	0.060	–1.04	2.11	3.17	–1.48

Table 1). The temperature dependences $\rho(T)$ observed for manganites at low temperatures can be explained in the framework of the double-exchange model [1, 4, 14, 16].

A strong electron–electron scattering, as a rule, leads to the term ρ_1 proportional to T^2. According to the Kubo calculations (see reviews [1, 4]), the scattering of electrons by magnons results in the term $\rho_2 \propto T^{4.5}$. The relationship $\rho_2 \propto T^{4.5}$ was actually observed for the $La_{0.67}Ba_{0.33}MnO_3$ manganite films deposited onto the LSAT(001) substrates [16]. Analysis of the temperature dependences of the resistance for our films on the log–log scale (Fig. 2) demonstrates that, in the low-temperature range 4.2–200 K, the dependence $\rho(T)$ is described with a high accuracy by the expression

$$\rho(T) = \rho_0 + \rho_1 T^n \quad (1)$$

with the exponent $n = 2.5 \pm 0.1$. The same expression was also observed for this material in [13, 14].

The relationship $\rho(T) \propto T^{4.5}$ [4] associated with the electron–magnon interaction does not describe the experimental dependence $\rho(T)$ but can modify the exponent in the temperature dependence. A recent theoretical analysis of the resistance of manganite films [18] showed that, owing to the double-exchange mechanism, the coupling between the static conductivity fluctuations and the spin fluctuations is responsible for the temperature dependence of the resistance $\rho(T) \propto T^{2.5}$, which is indeed observed in our experiment. However, the quantity ρ_1 in the experimental temperature dependence $\rho(T) \propto T^{2.5}$ appears to be one order of magnitude larger than that predicted by the theory [18].

In manganite films, the transition to the ferromagnetic state with a decrease in temperature at $T < T_C$ is accompanied by a changeover from a hopping behavior of the temperature dependence of the resistance to a metallic behavior at the temperature $T = T_p$.[3] As a rule, the temperature T_p coincides with the Curie temperature T_C to an accuracy of a few degrees. At temperatures in the vicinity of the Curie point T_C, the temperature and magnetic field dependences of the resistance are determined by the activation processes [19].

5. MAGNETO-OPTICAL CHARACTERISTICS OF FILMS

The magnetic characteristics of the LSMO films in the external magnetic field applied parallel to the plane of the sample were investigated using the meridional magneto-optical Kerr effect. The magnetization curves, the coercive force H_c, the saturation field H_s, and the anisotropy field H_a were determined at room temperature.

[3] The temperature T_p is determined from the maximum value of the resistance.

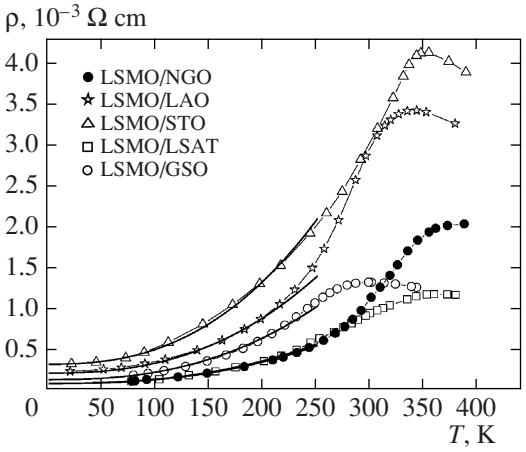

Fig. 2. Temperature dependences of the resistivity of the films. Solid lines indicate the approximations $\rho(T) = \rho_0 + \rho_1 T^{2.5}$. The parameters obtained for the approximation $\rho(T)$ from the analysis of the dependences $\rho(T)$ on a logarithmic scale are given in Table 2.

The behavior of the field dependences and the magnitude of the magneto-optical Kerr response for the LSMO films depend substantially on the substrate material (Fig. 3). No anisotropy of the magneto-optical Kerr response for the LSMO films on the LAO and STO substrates is observed upon rotation of the substrate around the normal to the substrate plane. The magnetization curves for the samples grown on the STO and LAO substrates are shown in Fig. 3a. Upon rotation of the samples around the normal to their surface, the shape of the curves remains unchanged, which indicates the absence of a preferred magnetization direction in the plane. A small value of the coercive force for the LSMO/STO structure (4–5 Oe) suggests that this system belongs to the class of "soft magnetic" materials. The magnetization of the LSMO/LAO films does not reach complete saturation in the external magnetic field with a strength of up to 1 kOe (see the inset to Fig. 3a). Most likely, this circumstance is associated with the occurrence of the easy magnetization axis deviating from the film plane [8]. The magneto-optical Kerr signal in the LSMO/GSO films is at the noise level due to the low Curie temperature ($T_C < 290$ K).

The LSMO/NGO film is characterized by a magnetic anisotropy of the easy-axis type as a function of the direction of the external magnetic field lying in the plane of the substrate. Upon magnetization along the easy axis, the magnetization curve exhibits a rectangular hysteresis loop when the coercive force $H_c = 15$ Oe coincides with the saturation field H_s. The inset to Fig. 3b shows the angular dependence of the saturation field H_s for the LSMO/NGO film. The magnetization along the hard axis is attended by the rotation of the magnetic moment in the plane of the sample, and the corresponding curve is characterized by a narrow (no more than 1 to 2 Oe) hysteresis loop. In this case, the

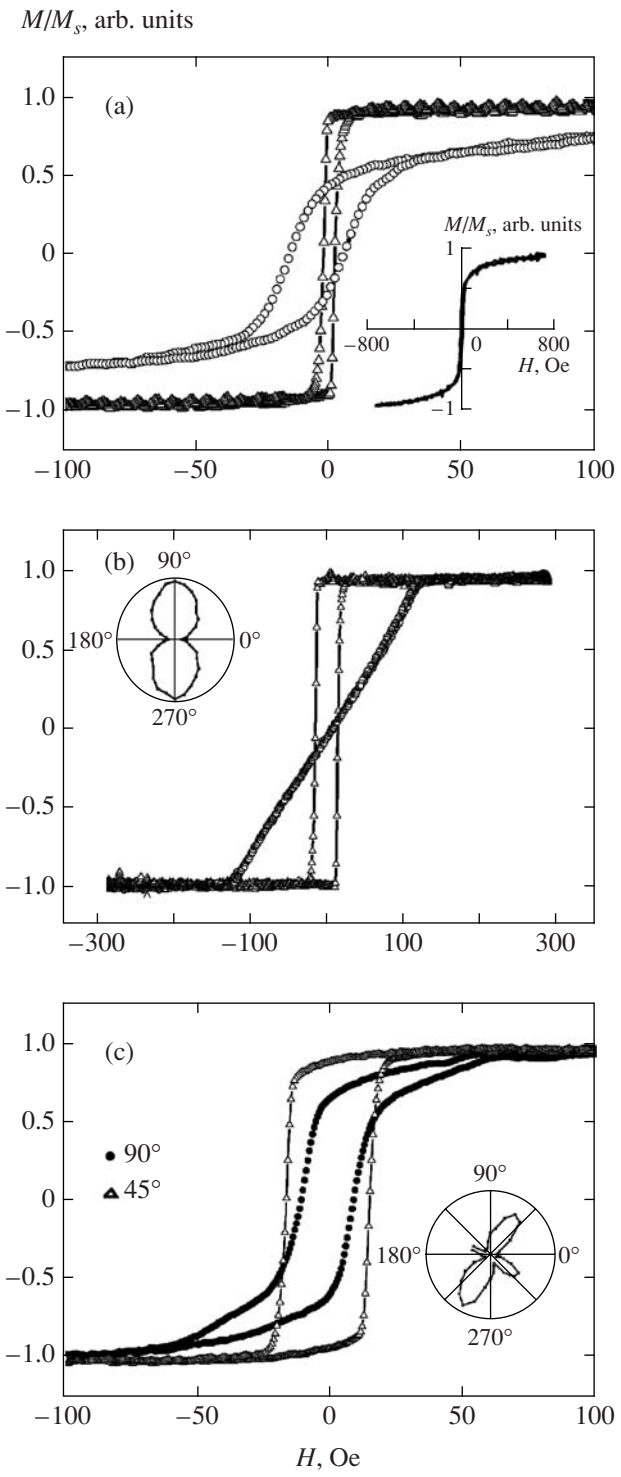

Fig. 3. Magnetization curves for the structures under investigation: (a) LSMO/STO (triangles), LSMO/LAO (circles), (b) LSMO/NGO, and (c) LSMO/LSAT films. In panels (b) and (c), triangles and circles correspond to different magnetic field directions. The inset to panel (a) shows the magnetization curve for the LSMO/LAO film on an enlarged scale with respect to the external magnetic field. The insets to panels (b) and (c) show the angular dependences of the saturation field H_s in the plane of the substrate for the LSMO/NGO and LSMO/LSAT films, respectively.

saturation field H_s is considerably higher than that upon magnetization along the easy axis; it is equal to the anisotropy field H_a and amounts to 120 Oe. The anisotropy of the magnetic properties of the LSMO/NGO films is probably associated with the crystallographic anisotropy of the NGO(110) plane of the substrate. The NGO substrate has an orthorhombic unit cell with the following parameters: $a = 0.5426$ nm, $b = 0.5503$ nm, and $c = 0.7706$ nm (see, for example, [17]). The parameter corresponding to the pseudocubic unit cell of the NGO substrate is equal to 0.3851 nm. A more accurate inclusion of orthorhombic distortions for the NGO(110) plane leads to anisotropy along the NGO[001] and NGO[110] directions (forming the NGO(110) plane): $2(a_{001} - a_{110})/(a_{001} + a_{110}) = 0.3\%$. This anisotropy is most likely responsible for 80% uniaxial anisotropy of the saturation field H_s (Fig. 3b). The crystallographic anisotropy in the LSMO/LSAT films is absent because the LSAT substrates in the temperature range 150–1200 K have cubic symmetry [20]. However, the dependences $H_s(\phi)$ for the LSMO/LSAT structures are characterized by the biaxial anisotropy (Fig. 3c) determined by the cubic structure of the LSMO crystal [21, 22].

6. MAGNETIC RESONANCE INVESTIGATION OF FILMS

The ferromagnetic resonance spectra were recorded in order to determine the paramagnetic–ferromagnetic transition temperatures and to study the in-plane magnetization anisotropy of the films. Figure 4 depicts the ferromagnetic resonance spectra at room temperature for the LSMO films grown on the substrates of four types. For each film, Fig. 4 shows two spectra that differ from each other by the rotation of the substrate through 90° around the normal to the substrate. It can be seen from Fig. 4 that the maximum change in the resonance magnetic field H_0 upon rotation of the sample by 90° is observed for the LSMO/NGO films.

The shape of all ferromagnetic resonance spectra at room temperature can be described by two Lorentzian lines. This fact uniquely indicates that the ferromagnetic phases in all films are inhomogeneous. Since the strain can gradually decrease with increasing thickness and the Curie temperature T_C and the g factor depend on the strain ε, two ferromagnetic phases most likely correspond to film layers with different strains. The difference between the g factors of the Lorentzian lines used for describing the experimental ferromagnetic resonance spectra does not exceed the width δ_{pp} of the ferromagnetic resonance line. The nonmagnetic layer, which, according to [9], is located at the film–substrate interface, does not substantially affect the ferromagnetic resonance.

Figure 5 shows the angular dependences of the resonance magnetic field H_0 for two films LSMO/NGO and LSMO/LSAT under investigation at room temperature upon rotation of the sample around the normal to

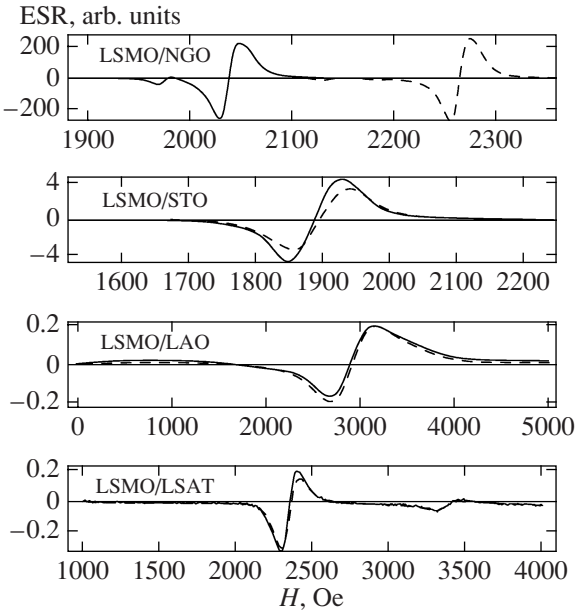

Fig. 4. Ferromagnetic resonance spectra of the four structures under investigation at room temperature for two mutually perpendicular orientations of the external magnetic field lying in the plane of the substrate (solid and dashed lines).

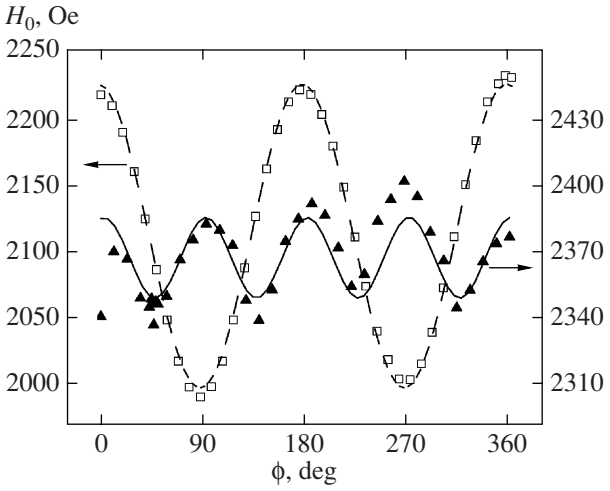

Fig. 5. The angular dependences of the resonance field H_0 for the LSMO/NGO (squares) and LSMO/LSAT (triangles) films upon rotation of the sample by the angle ϕ around the normal to the plane of the substrate. Solid and dashed lines correspond to the relationship $H_0 \propto 2H_1\cos(2\phi) + 2H_2\cos(4\phi)$ for constant quantities H_1 and H_2 fitted according to the best agreement with the experimental data.

the plane of the film. The constant magnetic field and the magnetic component of the microwave field lie in the plane of the film. Since the substrates with the film represent square plates 5×5 mm^2 in size, the influence of the shape anisotropy is minimum and the shift in the resonance field is completely determined by the magnetic anisotropy of the LSMO film. It can be seen from Fig. 5 that the angular dependence of the resonance field is well described by the relationship $H_0 \propto 2H_1\cos(2\phi) + 2H_2\cos(4\phi)$ with the amplitudes $H_1 = 55.8$ Oe and $H_2 = 0.9$ Oe for the LSMO/NGO film. For the LSMO/LSAT structure, we have $H_1 = 3.0$ Oe and $H_2 = 8.4$ Oe. It should be noted that the angular dependences of the magnetic anisotropy of the LSMO/NGO and LSMO/LSAT films are in good agreement with the corresponding dependences obtained from the magneto-optical measurements (see Section 5). The magnetic anisotropy of the LSMO film is determined by the combination of the cubic anisotropy (in the crystal) proportional to $K_1\sin4\phi$ and the anisotropy induced by the uniaxial strain $K_u\sin2\phi$ [21, 22]. According to the measurements performed in [22] for the LAO, STO, and MgO substrates, the quantity K_1 for the LSMO film decreases sharply with an increase in the temperature and the effect of the uniaxial strains K_u is almost independent of the temperature [22]. As a result, the influence of the cubic anisotropy of the LSMO structure at room temperature manifests itself only for the LSMO/LSAT films, for which the effect of the uniaxial anisotropy is minimum. With a decrease in the temperature, Tsui et al. [6] experimentally observed the biaxial anisotropy for the LSMO films deposited onto three substrates NGO, LSAT, and STO, which provide the minimum mismatch between the lattice parameters.

The temperature dependences of the resonance magnetic field for the three samples under investigation are plotted in Fig. 6. The paramagnetic–ferromagnetic transition temperature was identified as the abscissa corresponding to the inflection point of the above dependences. The Curie temperatures T_C thus determined are presented in Table 2.

The analysis of the ferromagnetic resonance spectra and their temperature dependences clearly indicates that there is a correlation between the ferromagnetic properties of the films and the crystallographic matching of the substrate and film materials. A comparison of the data presented in Tables 1 and 2 allows us to trace that a deterioration of the crystal quality results in an increase in the ferromagnetic resonance width δ_{pp}. However, at identical crystal quality (equality of the widths of peaks in the rocking curves), the Curie temperature T_C depends on the bulk strains [11]. It should be noted that the ferromagnetic resonance width $\delta_{pp} = 20$ Oe for our LSMO/NGO film is close to a record width for the epitaxial LSMO films.

Figure 7 shows the dependences of the Curie temperature T_C on the bulk and biaxial strains. The plane in the three-dimensional space describes the dependence

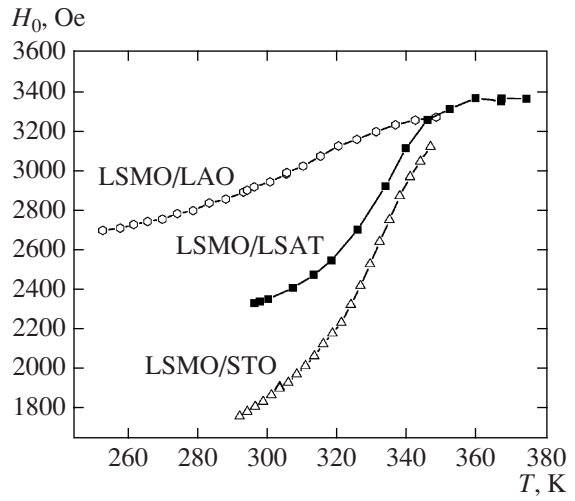

Fig. 6. Temperature dependences of the resonance magnetic field for three films (○) LSMO/LAO, (■) LSMO/LSAT, and (△) LSMO/STO. The Curie temperatures were determined from the maximum of the derivative dH_0/dT.

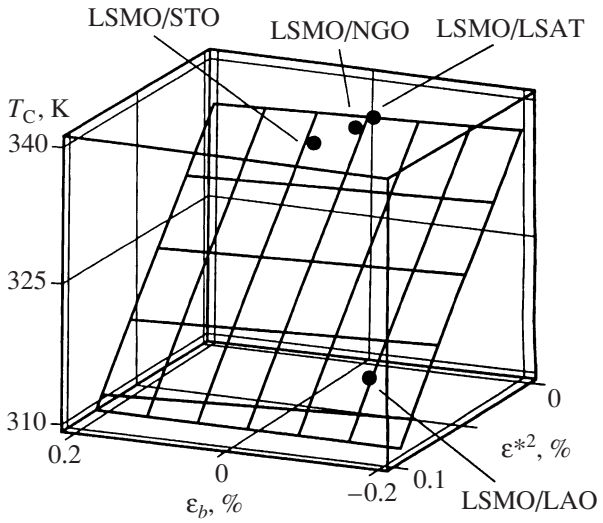

Fig. 7. Dependences of the Curie temperature T_C on the bulk strain ε_b and the square of the biaxial strain ε^{*2} for the LSMO films. The plane is constructed using relationship (2).

of the Curie temperature T_C on the arising strain according to the relationship obtained by Millis et al. [11]:

$$T_C(\varepsilon) = T_C(0)(1 - \alpha\varepsilon_b - \delta\varepsilon^{*2}/2), \qquad (2)$$

where $\alpha = (1/T_k)dT_C/d\varepsilon_b$ and $\delta = (1/T_C)d^2T_C/d\varepsilon^{*2}$. In our case, the best agreement between the experimental Curie temperature T_C and the temperature T_C^M in relationship (2) is achieved at $\alpha = 0.66 \pm 0.07$, $\delta = 103 \pm 2$, and $T_C(0) = 336 \pm 0.2$ K (see Table 2). A comparison of the calculated temperatures T_C^M and the experimental Curie temperatures T_C demonstrates that the deviation of the experimental Curie temperatures from the calculated temperatures is rather small (1 K) for the four most widely used substrates. The largest deviation observed for the Curie temperature T_C of the LSMO/GSO films is possibly associated with the considerable bulk distortions of the LSMO film. A higher defectiveness (larger width $\Delta\omega$) of the LSMO/GSO film leads to a broad ferromagnetic resonance line. It should be noted that the parameters obtained for relationship (2) that provide the best agreement between the theoretical and experimental data somewhat differ from those determined by Tsui et al. [6]: $\alpha = 2.2$, $\delta = 70$, and $T_C(0) = 334$ K.

7. CONCLUSIONS

Thus, epitaxial manganite films deposited onto six substrates providing compression and tension of the crystal lattice of the films were investigated. It was demonstrated that the temperature dependence of the resistance of all films at low temperatures is well described by the power relationship $T^{2.5}$, which follows from the results of recent calculations of the electrical conductivity of manganites in the framework of the double-exchange model. A weak anisotropy (on the order of 0.3%) of the NGO substrate leads to the observed anisotropy of the magnetic properties of the films in the plane of the substrate at room temperature. However, an insignificant crystallographic mismatch

Table 2. Electrical and magnetic characteristics of films

Substrate	ρ_0, Ω cm	ρ_1, Ω cm/$T^{2.5}$	H_c, Oe	H_s, Oe	T_C, K	T_C^M, K	δ_{pp}, Oe
NGO	0.82×10^{-4}	4.7×10^{-10}	15/<1*	120	335	335	65
LAO	2.12×10^{-4}	12×10^{-10}	10	100	315	316	340
STO	3.2×10^{-4}	18×10^{-10}	4	10	333	334	64
LSAT	0.85×10^{-4}	4.9×10^{-10}	10	50	336	336	100
GSO	1.3×10^{-4}	9.1×10^{-10}	–	–	251	328	330*

between the LSMO film and the LSAT substrate is responsible for the magnetic anisotropy typical of cubic ferromagnetic materials. The ferromagnetic resonance lines of all films are adequately described by a superposition of two Lorentzian lines, which indicate the presence of two ferromagnetic phases. The dependence of the Curie temperature determined from the ferromagnetic resonance spectra is qualitatively described by the Millis theory, which takes into account both the bulk and biaxial strain of the LSMO films.

ACKNOWLEDGMENTS

We would like to thank V.I. Atsarkin, Yu.A. Boĭkov, D. Winkler, A.L. Vlasyuk, T. Claeson, K.Y. Constantinyan, I.M. Kotelyanskii, Ya.M. Mukovskii, and A. V. Shadrin for helpful discussions of the results and for assistance in performing the investigations.

This study was performed within the programs "Strongly Correlated Electrons in Semiconductors, Metals, Superconductors, and Magnetic Materials" and "Spin-Dependent Effects in Solids and Spintronics" of the Branch of General Physics and Astronomy of the Russian Academy of Sciences; Program P-03-2.25 of the Presidium of the Russian Academy of Sciences; the Program of the European Union (project no. NMP3-CT-2006-033191); and the programs "Arrays of Quantum Dots and Josephson Junctions" and "Thin Films for Novel Oxide Devices" of the European Science Foundation; it also receive support from the International Science and Technology Center (project no. 3743); the Ministry of Education and Science of the Russian Federation; the Council on Grants from the President of the Russian Federation for the Support of Leading Scientific Schools (project no. NSh-5408.2008.2); and the Russian Foundation for Basic Research (project no. 08-02-00487).

REFERENCES

1. Yu. A. Izyumov and Yu. N. Skryabin, Usp. Fiz. Nauk **171** (2), 121 (2001) [Phys.—Usp. **44** (2), 109 (2001)].
2. W. Prellier, Ph. Lecoeur, and B. Mercey, J. Phys.: Condens. Matter **13**, R915 (2001).
3. A.-M. Haghiri-Cosnet and J. P. Renard, J. Phys. D: Appl. Phys. **36**, R127 (2003).
4. M. Ziese, Rep. Prog. Phys. **65**, 143 (2002).
5. P. Dey, T. K. Nath, and A. Tarapher, Appl. Phys. Lett. **91**, 012511 (2007).
6. F. Tsui, M. C. Smoak, T. K. Nath, and C. B. Eom, Appl. Phys. Lett. **76**, 2421 (2000).
7. Y. P. Lee, S. Y. Park, Y. H. Hyun, and J. B. Kim, Phys. Rev. B: Condens. Matter **73**, 224413 (2006).
8. Yan Wu, Y. Suzuki, U. Rüdiger, J. Yu, A. D. Kent, T. K. Nath, and C. B. Eom, Appl. Phys. Lett. **75**, 2295 (1999).
9. M. Bibes, S. Valencia, L. Balcells, B. Martĭnez, J. Fontcuberta, M. Wojcik, S. Nadolski, and E. Jedryka, Phys. Rev. B: Condens. Matter **66**, 134416 (2002).
10. H. Y. Hwang, T. T. M. Palstra, S.-W. Cheong, and B. Batlogg, Phys. Rev. B: Condens. Matter **52**, 15046 (1995).
11. A. J. Millis, T. Darling, and A. Migliori, J. Appl. Phys. **83**, 1588 (1998).
12. M. C. Martin, G. Shirane, Y. Endoh, K. Hirota, Y. Moritomo, and Y. Tokura, Phys. Rev. B: Condens. Matter **53**, 14285 (1996).
13. Yu. A. Boĭkov, T. Claeson, and V. A. Danilov, Fiz. Tverd. Tela (St. Petersburg) **47** (12), 2189 (2005) [Phys. Solid State **47** (12), 2281 (2005)].
14. G. J. Snyder, R. Hiskes, S. DiCarolis, M. R. Beasley, and T. H. Geballe, Phys. Rev. B: Condens. Matter **53**, 14434 (1996).
15. P. Schiffer, A. P. Ramirez, W. Bao, and S.-W. Cheong Phys. Rev. Lett. **75**, 3336 (1995).
16. Yu. A. Boĭkov and V. A. Danilov, Fiz. Tverd. Tela (St. Petersburg) **50** (1), 92 (2008) [Phys. Solid State **50** (1), 95 (2008)].
17. I. K. Bdikin, P. B. Mozhaev, G. A. Ovsyannikov, F. V. Komissinskiĭ, I. M. Kotelyanskiĭ, and E. I. Raksha, Fiz. Tverd. Tela (St. Petersburg) **43** (9), 1548 (2001) [Phys. Solid State **43** (9), 1611 (2001)].
18. M. J. Calderon and L. Brey, Phys. Rev. B: Condens. Matter **64**, 140403 (2001).
19. N. G. Bebenin, R. I. Zainullina, V. V. Mashkautsan, V. V. Ustinov, and Ya. M. Mukovskii, Phys. Rev. B: Condens. Matter **69**, 104434 (2004).
20. B. C. Chakoumakos, D. G. Schlom, M. Urbanik, and J. Luine, J. Appl. Phys. **83**, 1979 (1998).
21. Y. Suzuki, H. Y. Hwang, S.-W. Cheong, T. Siegrist, R. B. van Dover, A. Asamitsu, and Y. Tokura, J. Appl. Phys. **83**, 7064 (1998).
22. K. Steenbeck and R. Hiergeist, Appl. Phys. Lett. **75**, 17778 (1999).

Translated by O. Borovik-Romanova